JOURNAL OF COMPUTATIONAL PHYSICS 76, 233–242 (1988)

Finite Element Eigenvalues for the Laplacian over an L-Shaped Domain

B. SCHIFF

School of Mathematical Sciences, Raymond and Beverly Sackler Faculty of Exact Sciences, Tel Aviv University, Ramat Aviv, Tel Aviv, Israel

Received January 30, 1987

The standard finite element schemes for computing eigenvalues of the Laplacian converge slowly with decreasing mesh size if the domain boundary contains a re-entrant corner. A superelement is constructed to cover the region surrounding a corner of angle $3\pi/2$. Inside the superelement, the mesh is refined and the trial function constrained to fit the known analytic form of the solution in the neighborhood of the corner singularity. Being compatible with linear and bilinear elements, the superelement is easily embodied into standard finite element programs. Calculations are made for an L-shaped domain with various boundary conditions. Comparison with other calculations show that the incorporation of the superelement has neutralised the deterioration in convergence which would otherwise have taken place due to the presence of the re-entrant corner.

1. INTRODUCTION

It is often necessary to compute eigenvalues of the Laplacian subject to homogeneous conditions over the boundary of the domain considered. Two cases frequently encountered, for example, are the determination of the cutoff frequences for various modes of propagation in an electromagnetic waveguide [1], or of the frequences of vibration of an elastic membrane [2]. The computation is particularly difficult if the boundary contains one or more re-entrant corners. At each such corner, the solution has a singularity, and the usual computational schemes need to be modified. For finite element schemes, two main approaches have been adopted in order to enable them to deal with singularities in the solution. In one [3, 4], the finite element mesh is refined in the neighborhood of a singularity. In the other [5, 6], extra functions, which reflect the known analytic behavior of the solution in the neighborhood of the singularity, are included in the trial function basis. In the present paper, we describe a scheme which utilises both ideas. The singularity is surrounded by a "superelement" containing a refined mesh, over which the trial function is constrained to emulate the behavior of the analytic solution in the neighborhood of the singularity. The remainder of the domain is then covered with the usual elements. The method was first developed for problems in two-dimen-

0021-9991/88 $3.00

sional linear elasticity [7], the re-entrant corner arising as a result of a crack in the medium. In the work presently described, the method is adapted to solve an eigenvalue problem. Two superelements for a corner of angle $3\pi/2$, one with Dirichlet type homogeneous boundary conditions, and one with Neumann type, have been developed and applied to solve the eigenvalue problem for an L-shaped domain. Accurate results for such a domain with various types of boundary conditions have been obtained by other authors [5, 8–11], using a number of different methods, so that this may be regarded as a benchmark problem. The results currently obtained are in good agreement with those of previous calculations. The superelements may easily be incorporated into standard finite-element computational schemes, thus giving the method the advantage of general applicability.

The two superelements used in the current calculation have also been employed to compute cutoff frequencies for TE and TM modes in waveguides whose boundaries contain corners of angle $3\pi/2$, such as a cross-shaped guide, and guides containing ridges. The result of these calculations also agree well with those obtained by previous methods of less general applicability, and will be described elsewhere [12].

The method is outlined in Section 2 of this paper, and the results for an L-shaped domain are described in Section 3. The conclusions to be drawn from the calculations are outlined in Section 4.

2. The Computational Scheme

We wish to solve

$$\nabla^2 u + \lambda u = 0 \qquad \text{over } D$$

subject to boundary conditions

$$B(u) = 0 \qquad \text{on } \partial D,$$

where $B(u)$ may be u, $\partial u/\partial n$, or u over a part of ∂D and $\partial u/\partial n$ over the remainder. We consider the variational formulation of the problem, in which the solutions are the functions giving the Rayleigh quotient

$$R(v, v) = \frac{\iint_D \left[\left(\frac{\partial v}{\partial x} \right)^2 + \left(\frac{\partial v}{\partial y} \right)^2 \right] dx\, dy}{\iint_D v^2\, dx\, dy} \tag{1}$$

a stationary value when taken over all possible functions v which are sufficiently differentiable, and which satisfy the essential boundary conditions. The stationary values of $R(v, v)$ are the eigenvalues λ_k, and the corresponding functions u_k the eigenfunctions.

In the finite element method, the stationary values of the Rayleigh quotient are determined over a finite-dimensional subspace S^h of the space of admissible functions. A function $v^h \in S^h$ is expanded in the form $v^h = \sum_{j=1}^{n} q_j \phi_j(x, y)$, where $\phi_j(x, y)$ are the basis functions, usually of local support, and q_j, the generalised coordinates, are to be determined. On substituting this expression for v^h into the formula for $R(v, v)$ we obtain an expression of the form

$$R(v^h, v^h) = \frac{\mathbf{q}^T K^h \mathbf{q}}{\mathbf{q}^T M^h \mathbf{q}}, \tag{2}$$

where K^h and M^h are the stiffness and mass matrices, respectively, with elements

$$K_{ij}^h = \iint_D \left[\frac{\partial \phi_i}{\partial x} \frac{\partial \phi_j}{\partial x} + \frac{\partial \phi_i}{\partial y} \frac{\partial \phi_j}{\partial y} \right] dx\, dy$$

$$M_{ij}^h = \iint_D \phi_i \phi_j \, dx\, dy.$$

The stationary values of $R(v^h, v^h)$ are found by solving the generalised eigenvalue problem

$$K^h \mathbf{q} = \lambda^h M^h \mathbf{q}. \tag{3}$$

In the current method, we surround the singularity with a superelement, the construction of which will be described below, and use linear trial functions over triangles or bilinear functions over rectangles throughout the remainder of the domain. The construction of a superelement has been described in detail elsewhere [7] for a boundary value problem in elasticity. While the problem currently considered is an eigenvalue problem, the geometry of the superelement and the form of the trial functions is similar to that in the problem previously described. We will, therefore, confine ourselves to a brief description of the main features of the current method.

In constructing the superelement, we assume that the solution in the neighborhood of the singularity is of the form

$$u = \sum_{m=1}^{\infty} a_m f_m(r, \theta), \tag{4}$$

where $f_m(r, \theta)$ are known functions of the polar coordinates (r, θ) relative to an origin located at the singularity. The coefficients a_m are, of course, unknown, and the computation will yield approximate values for the first few coefficients.

The superelement contains two regions, an inner region D_{in} over which the mesh is refined, and a transition region D_{tr} which matches up between the refined mesh of D_{in} and the mesh in the region D_{out} outside the superelement. Over D_{in}, each original rectangular element is subdivided into n^2 smaller rectangles, where n will be

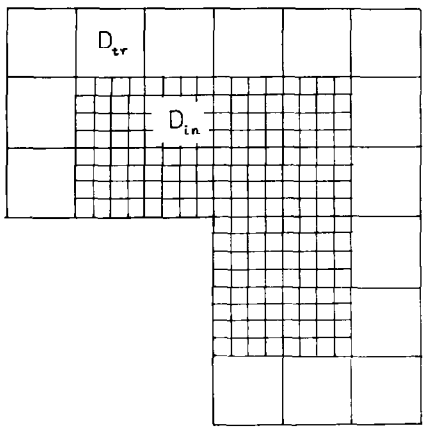

FIG. 1 L-shaped superelement with internal refinement ($n = 4$).

referred to as the internal refinement number. Figure 1 illustrates the form of an L-shaped superelement for the case $n = 4$.

In each small rectangle of D_{in}, we constrain the four nodal values to agree with the series (4), suitably truncated, at each corner, that is we require that

$$v^h(r_j, \theta_j) = \sum_{m=1}^{l} a_m f_m(r_j, \theta_j), \qquad j = 1, ..., 4. \tag{5}$$

The trial function over the small rectangle is then taken to be the bilinear interpolant to the values of the series (5) at the four corners. Thus the trial function over the whole of D_{in} will depend on the vector of coefficients $\mathbf{a} = (a_1, a_2, ..., a_l)$ alone. By assembling the stiffness and mass matrices for each small rectangle of D_{in}, we obtain the corresponding matrices for the whole region, expressed with respect to the vector of unknowns $\mathbf{a}$.

The trial functions over D_{tr} are designed to provide a smooth transition between the elements of D_{in} and D_{out}. Over a corner element of D_{tr}, a bilinear function is used, and it is constrained to agree with the series (5) at the corner adjoining D_{in}. A side element of D_{tr} is divided into n rectangular strips, and we use a piecewise bilinear trial function which linearly interpolates between the nodal values over the face abutting D_{out}, and is constrained to agree with the series (5) at each of the adjacent nodes of D_{in}. The unknowns over D_{tr} will thus be the vector of coefficients $\mathbf{a}$ together with the nodal values, i.e., the values of the trial solution, at the mesh points on the boundary of the superelement. We assemble the stiffness and mass matrices for the elements of D_{in} and D_{tr} to arrive at the superelement stiffness and mass matrices. These matrices need only be computed once for a given type of singularity with given boundary conditions.

Over D_{out}, we use linear trial functions over triangles, and bilinear or 5-point

hanging node bilinear functions [4] over rectangles. Thus the trial function is piecewise linear over the boundary of the superelement, hence conforming with the superelement trial function over its boundary. The stiffness and mass matrices for D_{out} are assembled in the usual way, and the previously calculated superelement matrices are added to obtain the global stiffness and mass matrices K^h and M^h for the whole domain. In contradistinction to the case described previously [7], it is not possible in our case to eliminate the unknowns **a** from the superelement matrix, as the relevant equations would involve the as yet unknown eigenvalue λ. Thus the variables to be finally solved for will be the nodal values at the mesh points of D_{out} (including those on the boundary of the superelement) together with the vector of coefficients **a**. Let us denote the vector of unknowns by **q**. Then we have to solve Eqs. (3) to obtain the eigenvalues λ_k^h and the corresponding eigenvectors $\mathbf{q}_k$ which will, of course, include the values of the coefficients a_m for the given eigenvalue λ_k.

3. Application to an L-Shaped Domain, Numerical Results

Following previous calculations, we took an L-shaped domain of size 2×2. The re-entrant corner was surrounded by a superelement of size 0.6×0.6, as shown in Fig. 2.

The basic mesh in the superelement was obtained by dividing each long side into six, so that each element of D_{tr} was of size 0.1×0.1. Over D_{out}, a coarse mesh of size 0.2×0.2 (mesh A) or a fine mesh of size 0.1×0.1 (mesh B) were used. In the former case, the superelement was surrounded with a single layer of elements of size 0.1×0.1, which were then joined to the elements of size 0.2×0.2 using 5-node hanging elements as depicted in Fig. 3.

For the series expansion (4), we used the solution appropriate to a re-entrant

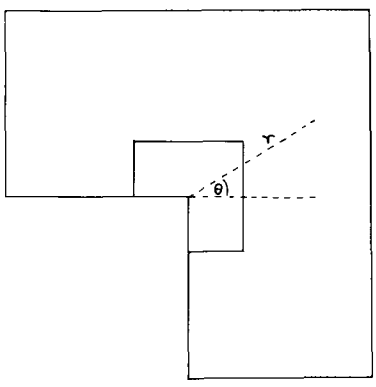

Fig. 2. Geometry of L-shaped domain with superelement.

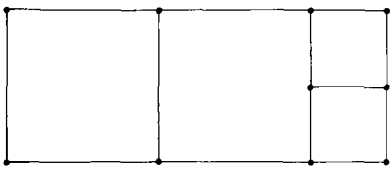

FIG. 3. Use of 5-node "hanging node" element.

corner of angle $3\pi/2$ in an infinite domain. For boundary conditions $u=0$ when $\theta=\pi$ and $\theta=-\pi/2$, the series is [5]

$$u=\sum_{i=0}^{\infty}\sum_{j=1}^{\infty} c_{ij}r^{2i+2j/3}\sin 2j\phi/3, \tag{6}$$

where $\phi=\pi-\theta$, whilst for the conditions $\partial u/\partial n=0$ over these same boundaries the series is

$$u=\sum_{i=0}^{\infty}\sum_{j=0}^{\infty} \gamma_{ij}r^{2i+2j/3}\cos 2j\phi/3. \tag{7}$$

The accuracy of the eigenvalues and eigenvectors will depend on the number of terms l in the truncated series, on the degree of mesh refinement in the superelement (that is, on the mesh refinement number n), and on the mesh size h in the region D_{out} external to the superelement.

After some experimentation, it was found that the inclusion of terms with a power of r higher than four made little difference to the results. We therefore included the terms $i=0; j=1, \ldots, 6$ and $i=1; j=1, 2, 3$, giving 9 terms in all, for the case of boundary conditions $u=0$ over the part of ∂D coinciding with the superelement boundary, while for the case $\partial u/\partial n=0$ we included the terms $i=0$; $j=0, \ldots, 6$, $i=1; j=0, \ldots, 3$, and $i=2; j=0$, a total of 12 terms in all.

In order to investigate the effect of refining the mesh inside the superelement, the superelement stiffness and mass matrices were computed with the values $n=2, 4, 8, 16$, and 32 for the mesh refinement number n, while including a fixed number of terms in the series expansion. The five values thus obtained for a given matrix element were used to determine the parameters a, b, c, p, q in an expression of the form $a+bn^{-p}+cn^{-q}$. The process was repeated for a number of different matrix elements, and in each case the values $p=2$ and $q=4$ were obtained almost exactly. We therefore computed extrapolated stiffness and mass matrices for the superelement by performing Richardson extrapolation [13] on each matrix element, assuming a dependence on n of the form $\sum_{k=1}^{4}\alpha_k n^{-2k}$, based on the values obtained for $n=2, 4, 8$, and 16. The extrapolated superelement matrices were employed in all of the subsequent calculations.

As regards the dependence of the results on the mesh size in the external region D_{out}, taking the results of [5, 8] for the $u=0$ boundary conditions as exact, we find

that the errors in the eigenvalues for mesh B (0.1×0.1) are very close to one quarter of those for mesh A (0.2×0.2). We therefore carried out one step of Richardson extrapolation, assuming an h^2 dependence for the errors, on the results for the two mesh sizes. The extrapolated values agree very well with the exact results.

In Table I, we tabulate the results for the boundary conditions $u = 0$, including the extrapolated values. For this case, Strang and Fix [14] obtained error bounds proportional to λ^2, the square of the eigenvalue, if linear or bilinear elements are used. We have, therefore, included the values of the error divided by λ^2 in the table, taking the results of [5, 8] as exact.

In Tables II and III we list our results, together with those of previous calculations for the case of $\partial u/\partial n = 0$, and for the case depicted in Fig. 4, in which $u = 0$ over one face and $\partial u/\partial n = 0$ over the remainder of the boundary. The extrapolated values were again obtained using h^2 extrapolation. The eigenvalues obtained are related to the cutoff frequencies for the propagation of electromagnetic waves in a symmetric ridged waveguide, the L-shape being half of the cross section, as illustrated in Fig. 4.

The boundary conditions $u = 0$ and $\partial u/\partial n = 0$ correspond to TM and TE waves, respectively. The values in Tables II and III are for TE waves which are symmetric and antisymmetric, respectively, about the middle of the cross section. The L-shaped domain shown in Fig. 2 is symmetric about the line $\theta = 45°$. Thus for

TABLE I

Eigenvalues Obtained with Boundary Conditions $u = 0$

	Mesh A		Mesh B				
k	λ	Error/λ^2	λ	Error/λ^2	Extrapolated λ	Exact λ	Dominant term
1	9 800	0.00173	9.695	0.00059	9.659	9.640[a, b]	$r^{2/3} \sin 2\phi/3$
2	15.606	0.00177	15.316	0.00051	15 219	15.197[b]	$r^{4/3} \sin 4\phi/3$
3	20.309	0.00146	19.901	0.00042	19 765	19.739[c]	$r^2 \sin 2\phi$
4	31.081	0.00179	29.958	0.00050	29.584	29.521[b]	$r^{4/3} \sin 4\phi/3$
5	33.643	0 00170	32.437	0 00051	32.035	31.913[a, b]	$r^{2/3} \sin 2\phi/3$
6	44.734	0.00190	42.531	0.00061	41.796	41.475[a, b]	$r^{2/3} \sin 2\phi/3$
7	48.662	0.00184	46.272	0.00065	45.476	44.949[b]	$r^{4/3} \sin 4\phi/3$
8	53.376	0.00165	50.713	0.00056	49.825	49.348[c]	$r^2 \sin 2\phi$
9	54.157	0.00197	50 733	0.00057	49.591	49.348[c]	$r^4 \sin 4\phi$
10	61.978	0.00164	58.148	0 00045	56.871	56 710[a, b]	$r^{2/3} \sin 2\phi/3$
11	72.147		67.470		65.911		$r^{4/3} \sin 4\phi/3$
12	81.659	0.00210	74.312	0.00064	71 863	71.059[a]	$r^{2/3} \sin 2\phi/3$
13	82.095		74.642		72 158		$r^{4/3} \sin 4\phi/3$
14	87.461	0.00136	81.472	0.00040	79.476	78.957[c]	$r^2 \sin 2\phi$
15	105 922	0.00208	94.229	0.00062	90.331	89.306[a]	$r^{2/3} \sin 2\phi/3$

[a] Ref. [5].
[b] Ref. [8].
[c] Eigenvalue of unit square.

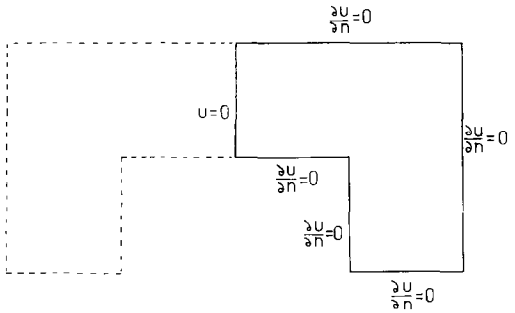

FIG 4. L-shaped domain as half of symmetric ridged guide cross section.

boundary conditions which are the same over the whole of ∂D the exact solution will be either symmetric or antisymmetric about this line, and the numerical results for the nodal values did indeed exhibit this symmetry. As a result of the symmetry, only certain terms in the series (6) or (7) have non-zero coefficients. In Tables I and II we list the form of the dominant term, i.e., the term with the lowest power of r for which a non-zero coefficient was obtained in the calculation. The case listed in Table III possesses, of course, no symmetry, because of the differing boundary conditions, and all of the series coefficients are different from zero.

The excellent agreement with the results of previous calculations show the errors in the eigenvalues to be of order h^2, as would have been obtained with linear or bilinear elements had no singularity been present [15]. Thus the introduction of the superelement has had the effect of neutralising the deterioration in the accuracy which would otherwise have occurred due to the presence of the singularity.

TABLE II

Eigenvalues Obtained with Boundary Conditions $\partial u/\partial n = 0$

k	Mesh A	Mesh B	Extrapolated	Previous calculations	Dominant term
1	1.486	1.479	1.476	1.516[a], 1.46[b]	$r^{2/3}\cos 2\phi/3$
2	3.564	3.542	3.534	3.539[a], 3.54[c]	$r^{4/3}\cos 4\phi/3$
3	10.122	9.943	9.884	9.869[a]	$r^2\cos 2\phi$
4	10.123	9.943	9.883	9.869[a]	1
5	11.677	11 469	11.399	11.38[c]	$r^{4/3}\cos 4\phi/3$
6	12.920	12.668	12.584	12.58[c]	$r^{2/3}\cos 2\phi/3$
7	20.246	19.877	19 754	19 7[c]	1
8	22.512	21.772	21.526		$r^{2/3}\cos 2\phi/3$
9	24.814	23.765	23.416	23.3[c]	$r^{4/3}\cos 4\phi/3$
10	29.920	28 884	28 538		$r^{2/3}\cos 2\phi/3$

[a] Ref. [9].
[b] Ref. [10]
[c] Ref. [11].

TABLE III

Eigenvalues Obtained with Mixed Boundary Conditions

k	Mesh A	Mesh B	Extrapolated	Previous calculations
1	0.31694	0.31648	0.3163	0.320[a], 0.31[b]
2	2.624	2.610	2.606	2.632[a], 2.59[b]
3	6.128	6.061	6.039	6 060[a]
4	10.461	10.280	10.220	10.209[a]

[a] Ref. [9].
[b] Ref. [10]

The computations for mesh A involved a total of 128 or 131 degrees of freedom (dof), including the series coefficients. The eigenvalues were obtained simultaneously using the IMSL routine EIGZS. For mesh B, 329 or 332 dof were employed, and the computation could not be carried out in core. Each eigenvalue, and the corresponding eigenvector, were calculated separately by inverse iteration [16].

The results of Fox *et al.* [8] are for the boundary condition $u=0$ and were obtained by collocating the exact series (6) over the domain boundary. For each symmetry type, only those terms in the series possessing the relevant symmetry were included, and the problem was solved over the unit square, the solution over the remaining two thirds of the domain being obtained from symmetry considerations. These authors obtained six-figure accuracy in the eigenvalues using only 26 dof. The object of the current calculation was to test the superelement for use over more general domains, and we therefore in each case included terms of all the symmetry types in the series and solved the problem over the whole domain.

The results of Fix *et al.* [5] were obtained using bicubic splines, augmented by up to 14 singular functions similar to those in (6) above, and their results agree with those of Fox *et al.* to six figures. A coarse and a fine mesh requiring 42 and 127 dof, respectively, were used. Bulley and Davies [9] employed a six-degree polynomial over each half of the L-shaped domain, imposing continuity of the function over the central line. They employed a total of 36 or 37 dof. The present method is, therefore, less efficient than the above-mentioned methods for the L-shaped domain, but is of more general applicability. The object of the current calculation was not to obtain results with maximum efficiency for this simple case, but rather to develop and test the accuracy of the superelement on a case where accurate results are available before applying it to more general domains, for which more specialised methods may not be available. The results of Beaubien and Wexler [10, 11] were obtained using standard finite differences. Their method is of general applicability, but requires a large number of dof (approximately 5000 for the L-shaped domain), as it makes no special provision for the singularity. The current

method, on the other hand, has been applied to a number of different domains [12], and satisfactory accuracy has been achieved in each case employing 150–420 dof.

4. Conclusions

The results of the present method are in excellent agreement with those obtained by other methods for an L-shaped domain, and also for other domains containing a re-entrant corner of angle $3\pi/2$. The superelement herein described thus facilitates the application of the finite element method to such domains, yielding eigenvalues of an accuracy comparable with that which would have been achieved had no re-entrant corner been present. The superelement may be easily incorporated into standard finite element programs and is compatible with linear or bilinear elements. In view of the availability of highly accurate results for domains containing a corner of angle $3\pi/2$, the method was tested on this case, but it is easily extended to the case of a corner of angle 2π, i.e., to domains containing a slit.

Acknowledgments

We are grateful to H. Yeshurun and D. Sagin for the use of their program BIGMATR for handling out-of-core matrix problems. IMSL routines were used for the in-core case. The computations were carried out on the CDC Cyber 855 at the Tel Aviv University Computation Center.

References

1. R E Collin, *Field Theory of Guided Waves* (McGraw-Hill, New York, 1960).
2. M G Milsted and J. R Hutchinson, *J. Sound Vib.* **32**, 327 (1974).
3. R Wait and A. R. Mitchell, *J. Comput. Phys* **8**, 45 (1971)
4. J. A. Gregory, D. Fishelov, B Schiff, and J R. Whiteman, *J. Comput Phys.* **29**, 133 (1978).
5. G. J. Fix, S. Gulati, and G I. Wakoff, *J Comput. Phys.* **13**, 209 (1973).
6. J. E Akin, *Intl. J Numer. Methods Eng.* **10**, 1249 (1976).
7. G Ogen and B Schiff, *J. Comput. Phys.* **51**, 65 (1983).
8. L. Fox, P. Henrici, and C. Moler, *SIAM J. Numer Anal.* **4**, 89 (1967).
9. R. M. Bulley and J. B Davies, *IEEE Trans. Microwave Theory Tech.* **MTT-17**, 440 (1969).
10. M. J. Beaubien and A. Wexler, *IEEE Trans. Microwave Theory Tech.* **MTT-18**, 1132 (1970).
11. M J Beaubien and A. Wexler, *Comput. J.* **14**, 263 (1971).
12. B. Schiff, *IEEE Trans. Microwave Theory Tech.*, submitted for publication.
13. A. Ralston, *A First Course in Numerical Analysis* (McGraw-Hill, New York, 1965), p. 120.
14. G. Strang and G. J Fix, *An Analysis of the Finite Element Method* (Prentice-Hall, Englewood Cliffs, NJ, 1973), p. 230.
15. G. Fix, *J. Math. Mech.* **18**, 645 (1969).
16. K. J. Bathe and E. L. Wilson, *Numerical Methods in Finite Element Analysis* (Prentice-Hall, Englewood Cliffs, NJ, 1976), p. 420.